Full Paper

Wiley Online Library

ELECTROANALYSIS

DOI: 10.1002/elan.201900190

Electrochemical Sensor Based on Multi-walled Carbon Nanotube/Gold Nanoparticle Modified Glassy Carbon Electrode for Detection of Estradiol in Environmental Samples

Milua Masikini,[a] Mariana Emilia Ghica,[b] Priscilla G. L. Baker,[a] Emmanuel I. Iwuoha,[a] and Christopher M. A. Brett*[b]

Abstract: We report a rapid and simple method for sensing estradiol by electro-oxidation on a multi-walled carbon nanotube (MWCNT) and gold nanoparticle (AuNP) modified glassy carbon electrode (GCE). Compared with a bare GCE, AuNP/GCE and MWCNT/GCE, the composite modified GCE shows an enhanced response to estradiol in 0.1 M phosphate buffer solution. Experimental parameters, including pH and accumulation time for estradiol determination were optimised at AuNP/MWCNT/GCE. A pH of 7.0 was found to be optimum pH with an accumulation time of 5 minutes. Estradiol was determined by linear sweep voltammetry over a dynamic range up to 20 % mol L^{-1} and the limit of detection was estimated to be 7.0×10^{-8} mol L^{-1}. The sensor was successfully applied to estradiol determination in tap water and waste water.

Keywords: estradiol oxidation · multi-walled carbon nanotubes · gold nanoparticles · electrochemical sensor · linear sweep voltammetry

1 Introduction

The group of steroid estrogen hormones, estrone (E1), estradiol (E2), and estriol (E3), Figure 1, are substances that promote the development and maintenance of female characteristics in the human body [1]. Of these, estradiol (E2), also called 17β-estradiol, is an endocrine disrupting chemical that can bring antagonistic impacts in the endocrine system of humans and wild animals. The introduction of estradiol into the body from outside, even at low concentrations, can lead to growth abnormalities and disturbs the functioning of the male reproductive system [2]. It represents a real danger to pre-mature puberty in children and increases the risk of breast and ovarian cancer in women [3]. Since E2 is a widespread medication for women, traces can exist in foods and in the environment. Trace levels of E2 can cause disequilibrium of humoral and cellular immunity, resulting in pathological changes to reproductive, immune, nerve and cardiovascular systems [3–5]. Estradiol is prescribed to women as medication in order to reduce symptoms of menopause, compensate low production of estrogen in hypogonadism, for hormonal birth control and as transgender hormone replacement therapy [6]. Consequently, a reliable, sensitive, selective and rapid method for the determination of estradiol in the organism, food or environment is of great importance.

Among the methods used to monitor estradiol: HPLC [4,7], surface plasmon resonance [8,9], fluorescence [10], Raman spectroscopy [11] etc., electrochemical techniques offer several advantages, such as short time of analysis, simplicity, high sensitivity and selectivity. In electrochemistry, the use of modified electrodes is very common; recent strategies for estradiol detection include different nanomaterials [12–14], molecularly imprinted polymers [3,15–17], and antibodies [18–21]. E2 has been determined at different electrodes, including hanging mercury [22], boron doped diamond [23], graphite [12,13] but predominantly glassy carbon with different modifiers: carbon nanotubes [12,24,25], graphene [14,26], nanoparticles [13,17,27], or polymers [2,28,29].

Among the nanomaterials, carbon nanotubes and gold nanoparticles are the most explored in the literature, due to their exceptional properties, which ensures a wide range of applications, in different areas such as electrocatalysis, separation, imaging [30]. CNTs have remarkable structural, electronic and magnetic properties, as well as high mechanical strength and electrical conductivity and have been used in electrochemical applications, e.g. [31,32]. Modification of electrodes by metal nanoparticles enhances the surface area-to-volume ratio [33,34] and

[a] M. Masikini, P. G. L. Baker, E. I. Iwuoha
SensorLab, Department of Chemistry, University of Western Cape, Robert Sobukwe Road, Bellville, Cape Town 7535, South Africa
[b] M. E. Ghica, C. M. A. Brett
Department of Chemistry, Faculty of Sciences and Technology, University of Coimbra, 3004-535 Coimbra, Portugal
E-mail: cbrett@ci.uc.pt

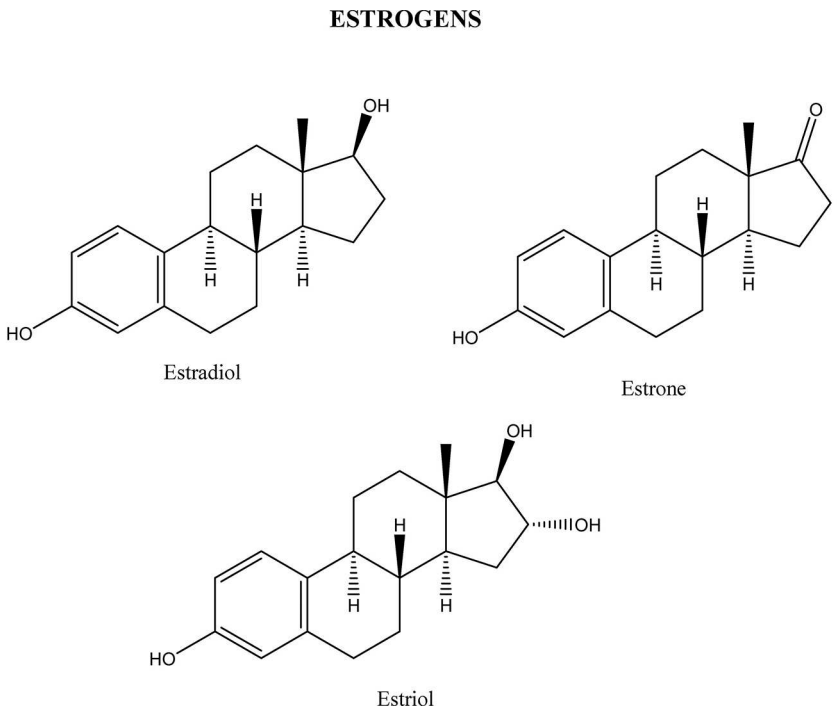

Fig. 1. Chemical structure of estrogens.

improves the electrochemical activity [33,35,36] through faster electron-transfer kinetics and consequent decrease in the overpotential required for the electrochemical response [33,37].

AuNP-CNT nanocomposites can be made by different methods and combine the excellent physical and chemical properties of both nanoparticles and nanotubes, with possible synergistic effects [30,38]. Direct deposition of AuNP onto CNT is easy and rapid to perform and the association between these materials offers various advantages for electrochemical sensing, among which are enhancement of selectivity and sensitivity, decrease of response time, reduction of the overpotential of analytes and improvement of stability [12,39].

The main objective of this work was to develop an easy to prepare, low-cost electrochemical sensor consisting of a glassy carbon electrode modified by AuNP/MWCNT nanocomposite for the detection of estradiol, a potential cancer agent. To our knowledge, there is only one study [12] in which the combination of MWCNT and AuNP for estradiol measurement has been used: a pencil graphite electrode was modified by layer-by-layer assembly, the assembly also containing polyethyleneimine and polyacrylic acid. Here, a less complex strategy for electrode modification is investigated. The performance of the resulting platform for estradiol sensing is compared with other sensors existing in the literature.

2 Materials and Methods

2.1 Reagents and Solutions

Multiwalled carbon nanotubes (MWCNT) diameter 30 ± 10 nm, 1–5 μm length and ~95 % purity, were obtained from Nanolab, USA. β-Estradiol, potassium hexacyanoferrate (II) trihydrate, sodium hydrogen phosphate, acetic acid, ethanol, $HAuCl_4$ and chitosan were obtained from Sigma-Aldrich, Germany. Di-sodium hydrogen phosphate dihydrate and potassium chloride were from Fluka, Switzerland. Sodium hydrogen phosphate and nitric acid were from Riedel-de Haën, Germany. Reagents were all analytical grade and used without further purification. Sodium phosphate buffer solutions (PB) pH 4.0 to 9.0 were prepared from 0.1 M sodium hydrogen phosphate and 0.1 M di-sodium hydrogen phosphate 2-hydrate. For pH adjustment, 5.0 M NaOH or 1.0 M HCl was used, as necessary. Standard potassium hexacyanoferrate (II) solutions, concentration 1.00 mM, were prepared by dissolving in 0.1 M potassium chloride electrolyte solution.

A 10 mM β-estradiol stock solution was prepared in ethanol. A 1 mM β-estradiol solution was prepared daily from this stock solution in a mixture of ethanol (40 %) and de-ionized water (60 %) followed by further dilution in 0.1 M phosphate buffer solution, used as supporting electrolyte, to give a 0.1 mM 17β-estradiol in 0.1 M PB solution. Millipore Milli-Q nanopure water (resistivity ≥ 18 MΩ cm) was used for preparation of all solutions. Experiments were performed at ambient temperature (25 ± 1 °C).

2.2 Instrumentation

The electrochemical experiments were performed using a computer-controlled potentiostat/galvanostat/ZRA (Gamry Instruments, Reference 600). An electrochemical cell, volume 5 mL, contained the gold nanoparticle/multi-walled carbon nanotube (AuNP/MWCNT) modified glassy carbon electrode (GCE) as working electrode, diameter 3 mm, a platinum wire auxiliary electrode and an Ag/AgCl (3 M KCl) electrode as reference.

A Crison 2001 micro pH-meter (Crison, Spain) was used for pH measurements.

The scanning electron microscopy (SEM) for the characterization of the nanostructured composite was a JEOL, JSM-5310, Japan and transmission electron microscopy (TEM) of the same nanostructures was carried out with a JEOL, JEM-1230. The experimental conditions were accelerating voltage 2.0 kV and working distance 4–5 mm for SEM and 200 kV accelerating voltage for TEM.

2.3 Functionalization of the Multi-walled Carbon Nanotubes and Gold Nanoparticles Synthesis

The functionalization of MWCNT was done in nitric acid as follows. A mass of 60 mg of MWCNT was added to 5 mL of a 3 M nitric acid solution and stirred for 24 h. The solid product was collected on a filter paper and washed several times with ultrapure water until the pH of the filtrate solution was close to neutral ($pH \approx 7$). The resulting functionalised MWCNT were then dried at 80 °C in an oven overnight. The dry MWCNT were dispersed in a solution of acetic acid 1 % (v/v) containing chitosan 1 % (m/v), a homogeneous and stable suspension of 2 mg/mL (0.2 %) being achieved after about 120 min of ultrasonication. The acid treatment leads to the presence of polar hydrophilic surface groups, such as carboxyl (–COOH), hydroxyl (–OH), quinone (–C(=O)), nitro ($–NO_2$), and amino groups ($–NH_2$) at the ends or at the sidewall defects of the nanotube structure [40–43]. A significant increase in the amount of carboxylic groups is obtained [43,44].

The gold nanoparticle (AuNP) dispersion was prepared as follows. A volume of 200 mL of a solution of 0.01 % $HAuCl_4$ in water was heated to boiling point, then 7.0 mL of 1.0 % $Na_3C_6H_5O_7$ was slowly added whilst stirring, allowed to react for 10 min and then left to cool to room temperature [45].

2.4 Fabrication of MWCNT and AuNP/MWCNT Modified GCE

Prior to preparation of the platform on the GCE, the electrode surface was polished with diamond spray (Kemet International, UK) on a polishing pad down to 3 μm particle size. The GCE was then rinsed with Milli-Q ultrapure water. Then, the unmodified electrode was successively cycled between 0.20 and 1.00 V at 100 $mV\,s^{-1}$ until stable cyclic voltammograms were obtained.

Following this, the sensor was prepared by drop coating an aliquot of MWCNT (3 μL) dispersion on the GCE surface by means of a micropipette and allowing to dry for 1 h at room temperature. For further modification by AuNP, if required, this was followed by drop coating 3 μL of AuNP and allowing it to dry for 30 min. This last procedure was repeated 5 times in order to get more AuNP on top of MWCNT, previously observed to be an optimum sensing configuration [46]. The GCE, modified with a film of MWCNT or of AuNP/MWCNT, was gently rinsed with Milli-Q ultrapure water before electrochemical measurements to remove loosely bound modifier. The MWCNT and AuNP/MWCNT modified GCE are denoted as MWCNT/GCE and AuNP/MWCNT/GCE, respectively.

2.5 Electrochemical Measurements

A volume of 5 ml of phosphate buffer solution (0.1 M, pH 7.0) was used as the supporting electrolyte for the electrochemical detection of estradiol. In a typical measurement procedure, AuNP/MWCNT/GCE was subjected to successive cyclic potential sweeps between 0.20 and 1.00 V at 100 $mV\,s^{-1}$ until stable cyclic voltammograms were obtained. Then, 10 μL of a solution of estradiol in ethanol was added to the supporting electrolyte and allowed to accumulate during 5 min at open circuit without stirring. A linear sweep voltammogram was then recorded from 0.20 to 1.00 V at 100 $mV\,s^{-1}$. After each measurement, the AuNP/MWCNT/GCE was conditioned by 5 successive cyclic voltammetric sweeps from 0.20 to 1.00 V at 100 $mV\,s^{-1}$ in phosphate buffer (PB) solution, which successfully removed any adsorbed estradiol.

2.6 Preparation of Waste Water Samples

Waste water samples, A and B, were collected from a water treatment plant located in Bellville South (Cape-Town city – South Africa). Sample A was a treated domestic waste water, treated using UV-vis irradiation. Sample B was a treated mixture of industrial and domestic waste water, the treatment using both UV-vis and biological methods also called bioreactor. A sample of tap water, C, was collected in the laboratory at the University of the Western Cape.

The waste waters were analysed in the following way. A selected volume (45 mL) of sample A, B or C was transferred to a centrifuge tube (50 mL). After this, 5 mL of supporting electrolyte (1.0 M, PB pH 7.0) was added to give a final volume of 50 mL. Then, 5 mL of this solution was transferred to the electrochemical cell and the measurement was carried out. Following this, the solution analysed was spiked with 50 %L of a standard solution of estradiol, and then stirred in order to homogenize the solution before a second electrochemical measurement. All solutions were freshly prepared just before the measurements.

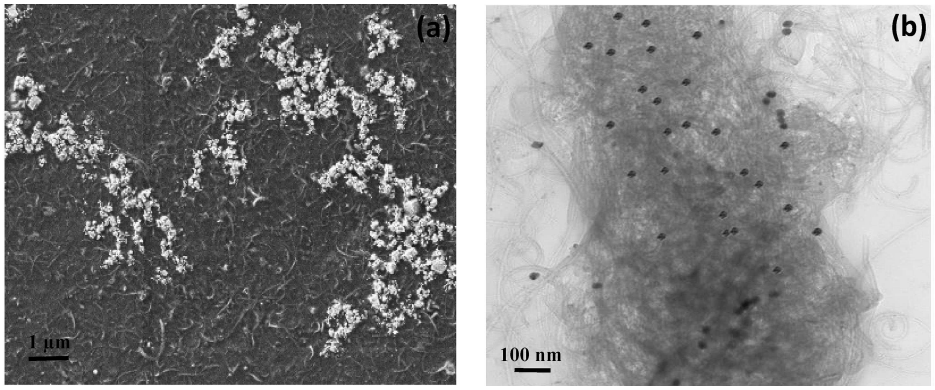

Fig. 2. (a) SEM and (b) TEM images of the CNT-AuNP nanostructures.

3 Results and Discussion

3.1 Characterization of Nanostructures

Structural and morphological characterization of the AuNP and CNT nanomaterial was performed by scanning and transmission electron microscopy. Figure 2a shows gold nanoparticles decorating carbon nanotubes. They are compactly attached to the walls of the nanotubes, suggesting the formation of a nanocomposite. The nanoparticles are well dispersed along the nanotubes and they exhibit spherical forms with diameters of ~20–30 nm, Figure 2b. The nanotubes were around 30 nm diameter with lengths of several micrometers, as expected, see Experimental Section.

3.2 Electrochemical Characterization of AuNP/MWCNT/GCE

The electrochemical performance of unmodified and modified GC electrodes, coated with MWCNT or AuNP/MWCNT, was probed by cyclic voltammetry (CV) in a solution of 1.0 mM potassium hexacyanoferrate (II) in 0.1 M KCl supporting electrolyte. Cyclic voltammograms are shown in Figure 3a. Compared with bare GCE, MWCNT/GCE and AuNP/MWCNT/GCE show higher peak currents and a small decrease in the values of peak potential. The increase in current response can be attributed to the greater electrochemically active surface area of the MWCNT/GCE and AuNP/MWCNT/GCE. The capacitive background currents were significantly higher at the MWCNT modified electrode than those at the unmodified electrode, expected when there is an increase in the available electrode surface area, and became more pronounced as each layer of AuNP is added. The shapes of the voltammograms of the modified and unmodified electrodes were slightly affected by the scan rate, and both anodic and cathodic peak currents show a linear dependence on the square root of the scan rate from 10 to 100 $mV\,s^{-1}$, so that the electrochemical process is diffusion-controlled [43]. The functional groups such as –COOH, –OH, and AuNP etc. of the modified electrode influence the rate of the electrode process [47].

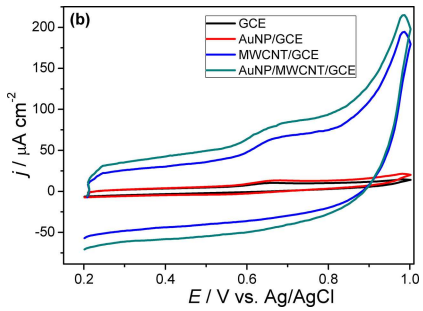

Fig. 3. Cyclic voltammograms of (a) 1.0×10^{-3} $mol\,L^{-1}$ $K_4[Fe(CN)_6]$ in 0.1 M KCl at (a1) GCE (a2) MWCNT/GCE and (a3) AuNP/MWCNT/GCE. Scan rate: 50 $mV\,s^{-1}$. (b) 1×10^{-5} $mol\,L^{-1}$ 17-β estradiol in 0.1 M phosphate buffer solution pH 7.0 after 5 min accumulation without stirring at GCE (black), AuNP/GCE (red), MWCNT/GCE (blue) and AuNP/MWCNT/GCE (green). Scan rate: 100 $mV\,s^{-1}$.

The electroactive area of the GCE, and modified electrodes MWCNT/GCE and AuNP/MWCNT/GCE, was estimated from the CVs at different scan rates from 10 to 100 $mV\,s^{-1}$, using the Randles-Sevcik equation for a reversible process: [43,48]. The slopes of I_{pa} versus $v^{1/2}$ plots for the oxidation process (data not shown) were: 3.674, 47.23×10^{-5} and 96.25×10^{-5} $A\,V^{-1/2}s^{1/2}$ for GCE, MWCNT/GCE and AuNP/MWCNT/GCE, respectively. Electroactive areas were thus estimated to be 0.054 cm^2, 0.705 cm^2 and 1.437 cm^2 for GCE, MWCNT/GCE and AuNP/MWCNT/GCE, respectively, the geometric area of the GCE being 0.071 cm^2. The incorporation of MWCNT and AuNP/MWCNT on the GCE increased the electroactive area by factors of 13.0 and 26.6 compared to the GCE, respectively, the composite AuNP/MWCNT giving a response twice higher than of the MWCNT modified electrode. This significant increase of electroactive area of AuNP/MWCNT/GCE compared to GCE and MWCNT/GCE is attributed to synergistic effects of the two nanomaterials (MWCNT and AuNP) used, both with high electrical conductivity and acting as a nanocomposite [49,50], as observed in SEM and TEM images, Figure 2.

3.3 Electrochemical Behaviour of Estradiol at Unmodified/Modified GCE

The electrochemical behaviour of 10 μmol L^{-1} 17-β estradiol at bare GCE, MWCNT/GCE, AuNP/GCE and AuNP/MWCNT/GCE in 0.1 M PB solution pH 7.0 was investigated by CV in the potential range from 0.2 to 1.0 V at 100 mV s^{-1}. As shown in Figure 3b, an oxidation peak appeared at unmodified GCE and at all modified GCE. No reduction peak was observed for any of the electrodes, unmodified or modified, in the reverse scan, indicating that the electrochemical process of E2 is totally irreversible, in agreement with previous work [2,3,17]. The oxidation peak height of E2 was highest at the AuNP/MWCNT/GCE, all the modified electrodes exhibiting better response than the bare GCE, important for sensing applications. The value of the oxidation peak potential of E2 was around 660 mV (vs. Ag/AgCl) at all electrodes. These potentials are lower than those of some MWCNT [24] or AuNP/MWCNT [12] sensors reported in the literature.

The oxidation peak current increased for all modified electrodes by a factor of 1.6 at AuNP/GCE, 2.7 at MWCNT/GCE and 4.1 at AuNP/MWCNT/GCE, mostly due to the increase in electrode surface area, with a significant increase in background capacitive current for both MWCNT/GCE and AuNP/MWCNT/GCE, due to the presence of MWCNT, as well as to an increase in conductivity and synergistic effects of the nanomaterials used.

When multiple cyclic scans were recorded, a gradual decrease in the oxidation peak was observed for all types of electrode (data not shown). This indicated the occurrence of adsorption phenomena, arising from the oxidative adsorbing products of E2. Adsorption has been found to control the oxidation process of estradiol at various different modified electrodes [13,14,26]. Electrode conditioning by successive cycling of the modified electrodes in buffer solution for 5 cycles removed the response to estradiol and restored the original response. All the voltammograms presented in this work refer to the first scan.

3.4 Optimization of Determination Conditions

In order to optimise the performance of AuNP/MWCNT/GCE in relation to the oxidation of E2, experimental conditions such as pH and accumulation time were investigated.

3.4.1 Effect of Accumulation Time

Since estradiol presents characteristics of accumulation by adsorption, the dependence of oxidation peak current of 10 μmol L^{-1} 17-β estradiol in 0.1 M phosphate buffer solution on accumulation time (0 to 6 min) was investigated at AuNP/MWCNT/GCE using cyclic voltammetry, see Figure 4. No peak current was observed until 1 min

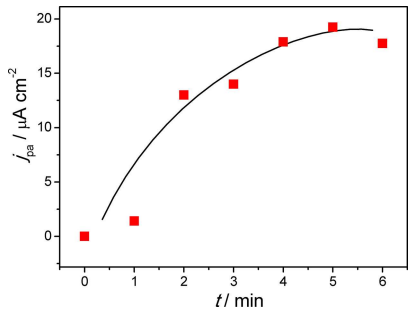

Fig. 4. Effect of accumulation time without stirring on the oxidation peak current of 1×10^{-5} mol L^{-1} 17-β estradiol in 0.1 M phosphate buffer solution pH 7.0 at AuNP/MWCNT/GCE.

accumulation time and the value of the oxidation peak current shows a large increase between 1 and 2 min. In the range studied, the response of E2 increased with increase of accumulation time between 1 and 5 min and reached a maximum at 5 min. When the accumulation time exceeded 5 min, the E2 oxidation peak current decreased, suggesting saturation of the estradiol adsorption sites. Thus, an accumulation time of 5 min was selected for the determination of E2, which is slightly higher than the 200 s [12] or 240 s [13,14] elsewhere; however, 4 min (240 s) is enough to ensure almost complete adsorption of E2 at AuNP/MWCNT/GCE, see Figure 4, and can also be used in order to reduce the measurement time. However, in order to maximize the response towards estradiol all the experiments performed in this study were conducted with a 5 min accumulation time.

3.4.2 Effect of pH Value

The effect of pH on the oxidation peak of 10 μmol L^{-1} 17-β estradiol in 0.1 M phosphate buffer solution at AuNP/MWCNT/GCE was studied using cyclic voltammetry in the pH range from 5.0 to 9.0 for 5 min adsorption time. As shown in Figure 5a, an increase in oxidation peak current was observed between pH 5.0 to pH 7.0, where the maximum was achieved, followed by a decrease for pH 8.0 and 9.0. Thus, the best response was obtained in pH 7.0 phosphate buffer solution, which was selected for further studies. This pH value was the choice for optimum estradiol detection by voltammetry with nanostructured architectures in other studies [14,26,51].

Figure 5b shows that the peak potential (E_p) is pH-dependent and progressively shifts to less positive potentials as the solution pH increases. A linear relationship between E_p and pH was obtained between pH 5 and 9, with a slope close to −50 mV per pH unit, close to the −59 mV corresponding to equal numbers of protons and electrons being involved in the electro-oxidation process of E2, as found in [26,51,25,48]. The possible mechanism of 17-β estradiol oxidation on AuNP/MWCNT modified glassy carbon electrode is presented in Figure 6.

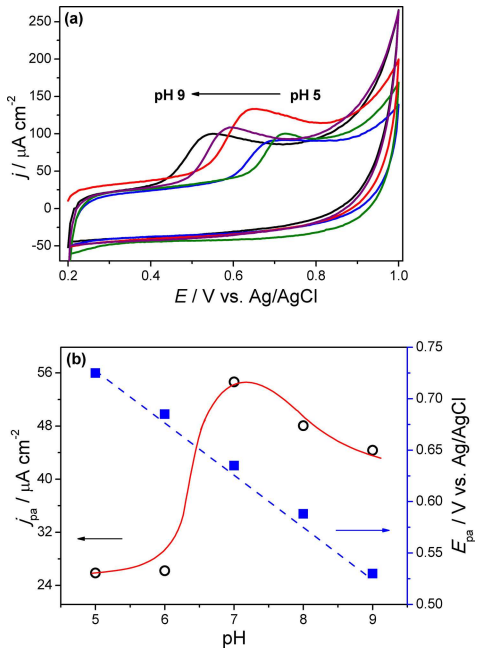

Fig. 5. (a) Cyclic voltammograms of 1×10^{-5} mol L^{-1} 17-β estradiol at AuNP/MWCNT/GCE at different pHs in 0.1 M PB solutions, scan rate 100 mV s^{-1}, accumulation time 5 min, no stirring, and (b) effect of the phosphate buffer solution pH on the oxidation peak current and potential.

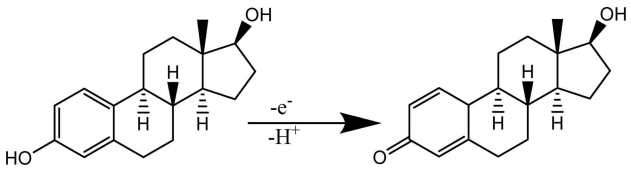

Fig. 6. Possible mechanism of 17-β estradiol oxidation on AuNP/MWCNT/GCE.

3.5 Performance of the AuNP/MWCNT/GCE Sensor

Linear sweep voltammetry (LSV) responses were used to quantify 17-β estradiol at the AuNP/MWCNT/GCE in 0.10 M PB solution. The use of linear sweep voltammetry was motivated by the fact that the electrochemical process of estradiol is irreversible and in order to minimise any fouling effect. It was found that differential pulse voltammetry does not lead to well-defined peaks, attributed to the effect of adsorption.

Under the optimized conditions, the relationship between oxidation peak current and concentration of 17-β estradiol was investigated, see Figure 7. The oxidation peak current of 17-β estradiol is linearly proportional to concentration over the range from 1 to 20 µmol L^{-1}. After 5-min accumulation and based on a signal-to-noise ratio determined from 3 experiments, the limit of detection was estimated to be 7.0×10^{-8} mol L^{-1} and the sensitivity to be 0.20 µA µM^{-1}. The detection limit was calculated as follows [52]:

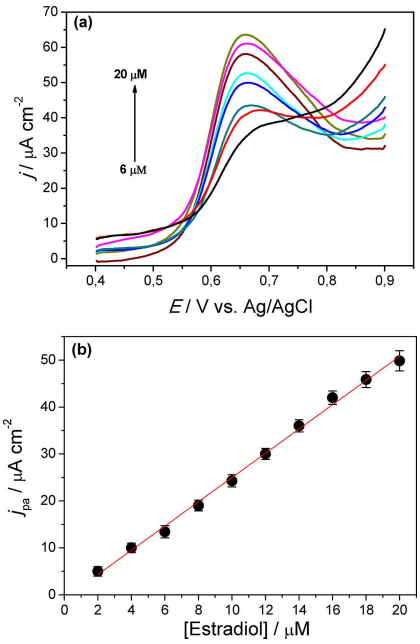

Fig. 7. (a) Typical linear sweep voltammograms at AuNP/MWCNT/GCE sensor for successive additions of 17-β estradiol in 0.1 M phosphate buffer solution pH 7.0. Scan rate: 100 mV s^{-1} and (b) corresponding calibration curve.

$$3xSD_{Blank}/S \quad (2)$$

with $SD_{(blank)}$ being a standard deviation of blank (for six measurements) and S the slope of the calibration plot.

Table 1 compares the AuNP/MWCNT/GCE sensor with other electrochemical sensor modified electrodes for detecting estradiol previously reported in the literature. The detection limit of 7.0×10^{-8} mol L^{-1} of the proposed sensor is significantly lower than that at a bare glassy carbon electrode (GCE) [53] and at a nanoPt-MWCNT/GCE [25], is similar to [2,14] but is higher than that reported for more complex and expensive modified electrode configurations, including PEDOT with gold nanocomposite aptasensor [21], carbon nanotube-ionic liquids [49], ordered mesoporous carbon with graphene [1] or poly(L-proline) [29] and molecularly imprinted polymers with gold nanomaterial [16].

3.6 Stability, Reproducibility and Selectivity

The stability of the AuNP/MWCNT/GCE sensor was investigated by LSV in PB containing 10 µmol L^{-1} 17-β estradiol. The sensor was stored at 4 °C for 5 days and measurements were made every day. The result shows that the sensor retained 79 % of its initial response after 5 days. The platform was stable on the surface of electrodes, so that the reduction in response may be due to some irreversible adsorption on the electrodes because of the high concentration of 17-β estradiol used in these experi-

Table 1. Comparison of the proposed sensor with other electrochemical sensorsfor estradiol detection.

Sensor	Dynamic range ($mol\,L^{-1}$)	Detection limit ($mol\,L^{-1}$)	Ref.
GR/OMC/CPE	5.0×10^{-9}–2.0×10^{-6}	2.0×10^{-9}	[1]
BPIDS/GCE	1.0×10^{-7}–1.0×10^{-5}	5.0×10^{-8}	[2]
$(AuNP\text{-}MWCNT)_n$/PGE	7.0×10^{-8}–4.2×10^{-5}	1.0×10^{-8}	[12]
RGO-DHP/GCE	4.0×10^{-7}–1.0×10^{-5}	7.7×10^{-8}	[14]
nanoPt-MWCNT/GCE	5.0×10^{-7}–1.5×10^{-5}	1.8×10^{-7}	[25]
PPOMC/GCE	1.0×10^{-8}–2.0×10^{-8}	5.0×10^{-9}	[29]
MWCNT-[bmim]PF_6/GCE	1.0×10^{-6}–7.5×10^{-6}	5.0×10^{-9}	[49]
GCE	4.0×10^{-5}–1.0×10^{-3}	1.0×10^{-5}	[53]
AuNP/MWCNT/GCE	1×10^{-6}–20×10^{-6}	7.0×10^{-8}	This work

GR/OMC/CPE: graphene ordered mesoporous carbon modified carbon paste electrode; BPIDS/GCE: poly{1-butyl-3-[3-(N-pyrrole) propyl]imidazoliumdodecylsulfonate} modified glassy carbon electrode; $(AuNP\text{-}MWCNT)_n$/PGE: pencil graphite electrode modified by gold nanoparticles-multiwalled carbon nanotube multilayers; RGO-DHP/GCE-glassy carbon electrode modified with reduced graphene oxide and dihexadecylphosphate; nanoPt-MWCNT/GCE: Pt nano-clusters/MWCNT modified GCE; PPOMC/GCE: poly(L-proline)-ordered mesoporous carbon composite modified glassy carbon electrode; MWCNT-[bmim]PF_6/GCE: GCE modified with MWCNT and an ionic liquid; GCE: glassy carbon electrode.

ments. The stability achieved with the proposed sensor is similar to that obtained in [25] with a glassy carbon electrode modified with Pt nanoclusters and MWCNT in which the sensor lost 25 % of its initial response to estradiol after 4 days. Better stability was reported in [2] at a GCE modified with electropolymerized ionic liquid, which lost only 9 % of its initial response to estradiol after 10 days. The reproducibility of the method was determined from the responses at five different AuNP/MWCNT/GCE sensors in the presence of 1×10^{-5} mol/L 17-β estradiol. A relative standard deviation of 1.7 % was obtained, indicating high reproducibility.

The effect of some potential interferents on the oxidation peak of 100 $\mu mol\,L^{-1}$ 17-β estradiol was investigated using LSV in the potential range of −0.2 to 1.0 V in 0.1 M PB pH 7.0. The environmental interferences used in this study include estrogens and heavy metal ions. The percentage values of current change in the presence of 20 $\mu mol\,L^{-1}$ 17-α ethynylestradiol (EE1), estriol (E3), estrone (E1) and equilin (EQ), were 14.2 %; 15.0 %; 17.4 % and 18.1 %, respectively, see Figure 8a. This can be explained by the similarity in the chemical structures of the compounds and electrochemical behaviour, their oxidation occurring at very similar potentials [1,25]; interference from estrone was also reported in [12]. In the case of heavy metal ions 50-fold higher concentrations of Pb^{2+}, Cu^{2+}, Cd^{2+}, Co^{2+}, Pd^{2+}, In^{2+}, Ni^{2+}, Bi^{3+}, Ge^{2+} and As^{3+} were tested. The current change was always less than 5 %, indicating no significant interference (Figure 8b).

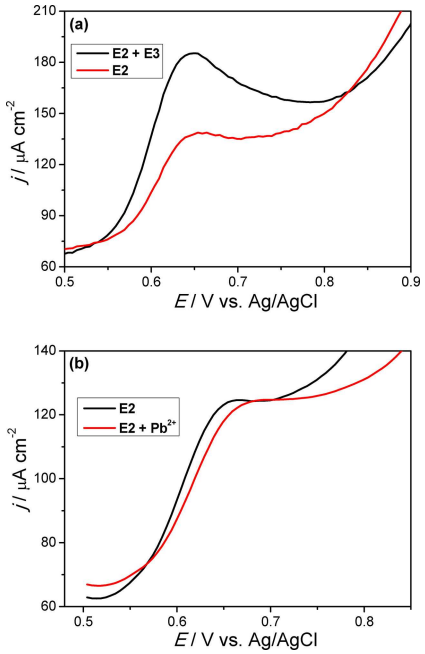

Fig. 8. Linear sweep voltammograms at AuNP/MWCNT/GCE sensor for 1×10^{-4} $mol\,L^{-1}$ 17-β estradiol (E2) in 0.1 M phosphate buffer solution pH 7.0 without and with (a) 2×10^{-5} $mol\,L^{-1}$ estriol and (b) 5×10^{-3} $mol\,L^{-1}$ Pb^{2+}.

3.7 Real Sample Analysis

In order to assess its applicability to real samples, the AuNP/MWCNT/GCE sensor was used to detect 17-β estradiol in two types of treated wastewater (A (domestic) and B (mixture of domestic and industrial)) and a tap water (C). The 17-β estradiol determinations were performed in triplicate, without any treatment procedure, employing the standard addition method. Recovery studies were performed by spiking 40 µL of standard solution (1×10^{-3} $mol\,L^{-1}$) in 5.0 ml of water samples prepared in 1.0 M phosphate buffer solution of pH 7.0, as explained above in the experimental section. The results obtained using LSV and the standard addition method are shown in Table 2. The percentage recovery was calculated from the total E2 concentration detected experimentally and the E2 concentration actually added to the samples. The recovery values obtained for 8×10^{-6} $mol\,L^{-1}$ concen-

Table 2. Recoveries for estradiol in water samples by the proposed method.

Water sample	Sample ($\mu mol\,L^{-1}$)	Amount Spiked ($\mu mol\,L^{-1}$)	Detected $\pm$SD[a] ($\mu mol\,L^{-1}$)	Recovery (%)	(%) RSD[b]
A (treated domestic wastewater)	N.D.[c]	8.00	7.88 ± 0.06	98.5	0.77
B (treated industrial + domestic wastewater)	N.D.[c]	8.00	7.58 ± 0.18	94.7	2.68
C (tap water)	N.D.[c]	8.00	7.87 ± 0.13	98.4	1.72

[a] SD: Standard deviation of three replicate determinations ($n=3$). [b] RSD: Relative standard deviation. [c] N.D.: Not detected

tration of 17-β estradiol in treated wastewater A and B, and tap water, C, fell in the ranges of 94.7–98.5 % and the RSD of all recovery experiments was less than 3 %, indicating that matrix effects do not pose any significant interference on the results.

4 Conclusions

In this work, a simple, easy to prepare and low cost electrochemical sensor has been proposed for the detection of estradiol. The AuNP/MWCNT/GCE electrochemical sensor shows a low detection limit, good stability and reproducibility and is demonstrated to be an excellent tool for the determination of estradiol in tap water and waste water samples. The results of the interference study show that the sensor can be used for the screening of the estrogens in waste water. Other modified electrode configurations with comparable analytical parameters have more complex architectures and are more expensive.

Acknowledgments

The authors gratefully acknowledge the financial support from the European Commission7th Framework Programme Marie Curie Actions People IRSES N°294993 SMARTCANCERSENS and Fundação para a Ciência e a Tecnologia (FCT), Portugal projects PTDC/QEQ-QAN/2201/2014, in the framework of Project 3599-PPCDT, and UID/EMS/00285/2013 (both co-financed by the European Community Fund FEDER). MEG thanks FCT for a postdoctoral fellowship SFRH/BPD/103103/2014. We are also grateful to the National Research Foundation (NRF) of South Africa for funding our research in South Africa and travelling grant.

References

[1] Y. Zhu, X. Liu, J. Jia, *Anal. Methods* **2015**, *7*, 8626–8631.
[2] Z. Wang, P. Wang, X. Tu, Y. Wu, G. Zhan, C. Li, *Sens. Actuators B* **2014**, *193*, 190–197.
[3] Q. Han, X. Shen, W. Zhu, C. Zhu, X. Zhou, H. Jiang, *Biosens. Bioelectron.* **2016**, *79*,, 180–186.
[4] Y. Shi, D. Peng, C. Shi, X. Zhang, Y. Xie, B. Lu, *Food Chem.* **2011**, *126*, 1916–1925.
[5] C. P. Silva, D. L. D. Lima, R. J. Schneider, M. Otero, V. I. Esteves, *J. Environ. Manage.* **2013**, *124*, 121–127.
[6] H. Kuhl, *Climacteric* **2005**, *8*, 3–63.
[7] B. Yilmaz, Y. Kadioglu, *Arab. J. Chem.* **2017**, *10*, S1422–S1428.
[8] Y. Cao, M. T. McDermott, *Anal. Biochem.* **2018**, *557*, 7–12.
[9] X. Du, L. Dai, D. Jiang, H. Li, N. Hao, T. You, H. Mao, K. Wang, *Biosens. Bioelectron.* **2017**, *91*, 706–713.
[10] H. Huang, S. Shi, X. Gao, R. Gao, Y. Zhu, X. Wu, R. Zang, T. Yao, *Biosens. Bioelectron.* **2016**, *79*, 198–204.
[11] S. Liu, R. Cheng, Y. Chen, H. Shi, G. Zhao, *Sens. Actuators B Chem.* **2018**, *254*, 1157–1164.
[12] G. Hao, D. Zheng, T. Gan, C. Hu, S. Hu, *J. Exp. Nanosci.* **2011**, *6*, 13–28.
[13] A. Özcan, D. Topçuogullari, *Sens. Actuators B Chem.* **2017**, *250*, 85–90.
[14] B. C. Janegitz, F. A. dos Santos, R. C. Faria, V. Zucolotto, *Mater. Sci. Eng. C* **2014**, *37*, 14–19.
[15] A. A. Lahcen, A. A. Baleg, P. Baker, E. Iwuoha, A. Amine, *Sens. Actuators B Chem.* **2017**, *241*, 698–705.
[16] X. Zhang, Y. Peng, J. Bai, B. Ning, S. Sun, X. Hong, Y. Liu, Y. Liu, Z. Gao, *Sens. Actuators B Chem.* **2014**, *200*, 69–75.
[17] A. Florea, C. Cristea, F. Vocanson, R. Sandulescu, N. Jaffrezic-Renault, *Electrochem. Commun.* **2015**, *59*, 36–39.
[18] X. Liu, P. A. Duckworth, D. K. Y. Wong, *Biosens. Bioelectron.* **2010**, *25*, 1467–1473.
[19] I. Ojeda, J. López-Montero, M. Moreno-Guzmán, B. C. Janegitz, A. González-Cortés, P. Yáñez-Sedeño, J. M. Pingarrón, *Anal. Chim. Acta* **2012**, *743*, 117–124.
[20] M. J. Monerris, F. J. Arévalo, H. Fernández, M. A. Zon, P. G. Molina, *Sens. Actuators B Chem.* **2015**, *208*, 525–531.
[21] R. A. Olowu, O. Arotiba, S. N. Mailu, T. T. Waryo, P. Baker, E. Iwuoha, *Sensors* **2010**, *10*, 9872–9890.
[22] S. Hu, Q. He, Z. Zhao, *Analyst* **1992**, *117*, 181–184.
[23] P. Gan, R. G. Compton, J. S. Foord, *Electroanalysis* **2013**, *25*, 2423–2434.
[24] Y. Sun, K. Wu, S. Hu, *Microchim. Acta* **2003**, *142*, 49–53.
[25] X. Lin, Y. Li, *Biosens. Bioelectron.* **2006**, *22*, 253–259.
[26] F. C. Moraes, B. Rossi, M. C. Donatoni, K. T. de Oliveira, E. C. Pereira, *Anal. Chim. Acta* **2015**, *881*, 37–43.
[27] G. C. Mauruto de Oliveira, E. P. de Palma, M. H. Kunita, R. A. Medeiros, R. de Matos, K. R. Francisco, B. C. Janegitz, *Electroanalysis* **2017**, *29*, 2638–2645.
[28] J. Song, J. Yang, X. Hu, *J. Appl. Electrochem.* **2008**, *38*, 833–836.
[29] L. Luo, F. Li, L. Zhu, Y. Ding, D. Deng, *Sens. Actuators B* **2013**, *187*, 78–83.

[30] S. Alim, J. Vejayan, M. M. Yusoff, A. K. M. Kafi, *Biosens. Bioelectron.* **2018**, *121*, 125–136.
[31] M. Masikini, S. N. Mailu, A. Tsegaye, C. O. Ikpo, N. Njomo, T. T. Waryo, P. G. L. Baker, E. I. Iwuoha, *Int. J. Electrochem. Sci.* **2014**, *9*, 7003–7020.
[32] G. A. Rivas, M. D. Rubianes, M. C. Rodriguez, N. F. Ferreyra, G. L. Luque, M. L. Pedano, S. A. Miscoria, C. Parrado, *Talanta* **2007**, *74*, 291–307.
[33] A. Maringa, E. Antunes, T. Nyokong, *Electrochim. Acta* **2014**, *121*, 93–101.
[34] F. W. Campbell, R. G. Compton, *Anal. Bioanal. Chem.* **2010**, *396*, 241–259.
[35] Y. Hu, Y. Song, Y. Wang, J. Di, *Thin Solid Films* **2011**, *519*, 6605–6609.
[36] M. Etesami, F. S. Karoonian, N. Mohamed, *J. Chin. Chem. Soc.* **2011**, *58*, 688–693.
[37] X. Huang, Y. Li, Y. Chen, L. Wang, *Sens. Actuators B* **2008**, *134*, 780–786.
[38] R. Y. Zhang, H. Olin, *Int. J. Biomed. Nanosci. Nanotechnol.* **2011**, *2*, 112–135.
[39] T. M. B. F. Oliveira, S. Morais, *Appl. Sci.* **2018**, *8*, 1–18.
[40] X. Jiang, J. Gu, X. Bai, L. Lin, Y. Zhang, *Pigm. Resin Technol.* **2009**, *38*, 165–173.
[41] L. Wang, S. Feng, J. Zhao, J. Zheng, Z. Wang, L. Li, Z. Zhu, *Appl. Surf. Sci.* **2010**, *256*, 6060–6064.
[42] Y. Shirazi, M. A. Tofighy, T. Mohammadi, A. Pak, *Appl. Surf. Sci.* **2011**, *257*, 7359–7367.
[43] F. C. Vicentini, B. C. Janegitz, C. M. A. Brett, O. Fatibello-Filho, *Sens. Actuators B* **2013**, *188*, 1101–1108.
[44] B. C. Janegitz, L. H. Marcolino-Junior, S. P. Campana-Filho, R. C. Faria, O. Fatibello-Filho, *Sens. Actuators B* **2009**, *142*, 260–266.
[45] V. Shakila, K. Pandian, *J. Solid State Electrochem.* **2007**, *11*, 296–302.
[46] N. Ben Messaoud, M. E. Ghica, C. Dridi, M. Ben Ali, C. M. A. Brett, *Sens. Actuators B Chem.* **2017**, *253*, 513–522.
[47] Y. Z. Song, Y. Song, H. Zhong, *Gold Bull.* **2011**, *44*, 107–111.
[48] D. Martín-Yerga, E. C. Rama, A. C. García, *J. Chem. Educ.* **2016**, *93*, 1270–1276.
[49] H. Tao, W. Wei, X. Zeng, X. Liu, X. Zhang, Y. Zhang, *Microchim. Acta* **2009**, *166*, 53–59.
[50] M. Tunckol, J. Durand, P. Serp, *Carbon* **2012**, *50*, 4303–4334.
[51] J. Li, J. Jiang, D. Zhao, Z. Xu, M. Liu, P. Deng, X. liu, C. Yang, D. Qian, H. Xie, *J. Alloys Compd.* **2018**, *769*, 566–575.
[52] A. Shrivastava, V. B. Gupta, *Chron. Young Sci.* **2011**, *2*, 21–25.
[53] B. Salci, I. Biryol, Voltammetric investigation of β-estradiol, *J. Pharm. Biomed. Anal.* **2002**, *28*, 753–759.

Received: March 21, 2019
Accepted: May 24, 2019
Published online on ■■, ■■

FULL PAPER

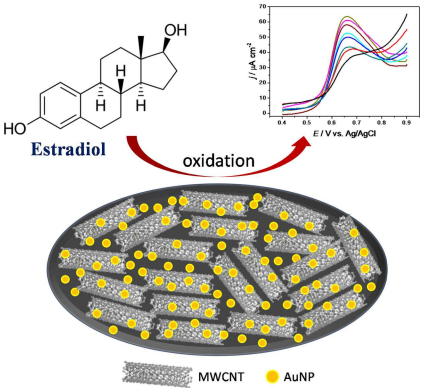

*M. Masikini, M. E. Ghica, P. G. L. Baker, E. I. Iwuoha, C. M. A. Brett**